

LEAF AREA INDEX ESTIMATES OBTAINED FOR MIXED FOREST USING HEMISPHERICAL PHOTOGRAPHY AND HYMAP DATA

Anja Visscher von Arx*, Silvia Huber, Mathias Kneubühler and Klaus Itten

Remote Sensing Laboratories (RSL), University of Zurich, Winterthurerstrasse 190, 8057 Zurich, Switzerland -
avissche@geo.unizh.ch

KEY WORDS: Hemisfer, Camera Exposure, Hyperspectral Data, Vegetation Indices, HyMap

ABSTRACT:

The Leaf Area Index (LAI) is an important measure in many ecological applications because vegetation-atmosphere processes of the canopy, such as photosynthesis are controlled by the foliage and play an essential role in the carbon cycle. Therefore accurate determination of LAI is of great interest. Forest LAI is difficult to estimate due to the complex structure of the canopy and its high variability. Previous studies have shown that hemispherical photography is a useful technique to determine LAI by involving different gap fraction models but exposure seems to affect LAI estimates. Hemispherical photography and LAI-2000 plant canopy analyzer ground measurements were taken to capture the LAI at selected plots in the study site. The photographs were captured with two different exposure settings, namely manual and automatic, to examine the effects on LAI. Subsequently, we analyzed the photographs with the Software Hemisfer that allows the calculation of LAI with five different mathematical methods. Hemisfer was developed by the Swiss Federal Research Institute WSL. In order to obtain an LAI map of the study area, data of the airborne imaging spectrometer HyMap were used, acquired in summer 2004. Three images were recorded approximately at the same time, whereas two of them were North-South oriented and the third perpendicular to them. All HyMap data were preprocessed and across-track illumination variations were corrected. Six two-band Vegetation indices (eg. PVI, SAVI2) were exploited by developing regression models between ground-based LAI and VI's. The VI with the best performance was then applied on HyMap data. The objectives of this study were (1) the evaluation of different mathematical methods to calculate LAI from hemispherical photographs, (2) the investigation of camera exposure influencing LAI estimates and (3) the examination of illumination effects on LAI when applying VI's on HyMap data. The evaluation of the five different LAI calculation methods from hemispherical photographs showed that the coefficients of variation ranged from 10.69 % to 15.43 %. LAI derived with manual camera exposure settings correlated better ($R^2=0.97$) with LAI-2000 values than LAI from automatically exposed photographs ($R^2=0.85$). A comparison of the VI's showed that good results were achieved with SAVI2 as well as with PVI. Investigating illumination effects on LAI indicated that although a correction has been performed, influences on LAI can still be observed.

1. INTRODUCTION

In forest ecosystems physical and biogeochemical processes take place. These processes are influenced by the microclimate within and outside of the canopy as well as by other factors. Biogeochemical processes such as photosynthesis, respiration or transpiration are controlled by the plants' foliage. In most studies canopy foliage is measured with the variable Leaf Area Index (LAI) (Chen and Cihlar, 1995; van Gardingen et al., 1999; Zhang et al., 2005). Leaf area index (LAI) is a dimensionless parameter and defined as the one-sided leaf area per ground surface area (Chen and Black, 1992). Since LAI plays a key role in ecological applications accurate determination of LAI is of great interest.

Forest LAI is difficult to estimate due to the complex structure of the canopy and its high variability. LAI can be estimated either directly or indirectly. Since direct methods, which involve destructive sampling or litterfall collection, are time consuming and limited to small areas, indirect techniques were developed. Indirect techniques include optical instruments, such as hemispherical photography or LAI-2000 Plant Canopy Analyzer that allow a non-destructive, quick and low-cost estimation of LAI over large areas (Chen et al., 1997). Previous studies have shown that digital hemispherical photography is a useful technique to determine LAI by

involving different gap fraction models. However, camera exposure settings influence the estimation of light transmission on LAI and are therefore a major cause of measurement errors (Zhang et al., 2005).

Since field estimations over large areas are problematic, remote sensing techniques have been used to measure LAI on a landscape scale (Gong et al., 2003). The most commonly used method to derive LAI of remote sensing data is the application of vegetation indices (VI's) by establishing empirical relationships between the ground-based LAI and the VI values.

The objectives of this study were (1) to evaluate five different mathematical methods to derive LAI from hemispherical photographs, (2) to investigate the effect of camera exposure on LAI and (3) to examine the illumination effects in HyMap images on LAI.

2. DATA ACQUISITION AND METHODS

2.1 Study Area and Sampling Design

Measurements were conducted in a mixed forest stand located in the Swiss Plateau close to the village of Vordemwald (47°16' N, 7°53' E). It covers about 60 km² at an altitude ranging from around 450 to 600 m above sea level. At the study area 15 subplots were determined, dominated mainly by European beech

* Corresponding author.

(*Fagus sylvatica* L.), European ash (*Fraxinus excelsior* L.), black alder (*Alnus glutinosa*), silver fir (*Abies alba*) and Norway spruce (*Picea abies* L).

The sampling design for each subplot was chosen according to the elementary sampling units of the VALERI project (Baret et al., 2006). For each subplot nine field measurements were collected on the basis of a 3 x 3 grid covering an area of 10 m by 10 m to average out errors in the levelling of the camera (Leblanc et al., 2005). Each subplot was located using GPS and marked for repeatable measurements. Data collections were carried out during the summer months of the years 2005 and 2006. In 2005, measurements were conducted at nine subplots under overcast weather conditions, whereas in 2006 data were acquired at five subplots under cloud free conditions. At four subplots measurements were carried out in both years.

2.2 Field LAI Data and Analysis

Field LAI were obtained with hemispherical photography and a Li-Cor LAI-2000 plant canopy analyzer (LI-COR, 1992). These two indirect optical methods allow a fast, inexpensive and non-destructive sampling. Both instruments retrieve LAI from gap fraction analysis. Chen and Black (1992) described LAI estimates derived with optical instruments as effective LAI. This term implies that also non-photosynthetically active plant elements are considered. However, in this study we use the term LAI.

Hemispherical photographs were collected using a Nikon CoolPix 4500 digital camera with a FC-E8 fish-eye lens (Nikon Inc., 2002). The photographs were taken looking upward by keeping the lens horizontal. An advantage of photographs compared to other methods is that they serve as a permanent record of the geometry and canopy openings (Rich, 1990). In order to understand how camera exposure settings affect LAI estimates, two different settings were used: first, the camera was set to automatic exposure and secondly, the aperture was fixed at F5.3 and only shutter speed was adjusted manually by considering the integrated photometer. Finally, at each subplot nine photographs which were either automatically or manually exposed were collected. We used the highest image quality (2272x1704 pixels) for all measurements and saved them in JPEG format. Photographs in this format have three image channels in the red, green and blue part of the electromagnetic spectrum.

All photographs were analyzed with the software Hemisfer, developed at the Swiss Federal Institute for Forest, Snow and Landscape Research (WSL) (Schleppi et al., 2006). Hemisfer derives LAI from the distribution of the gap fraction which was estimated using an overlay of five concentric rings covering the hemispherical photograph (van Gardingen et al., 1999). The gap fractions were determined by setting an automatic threshold which recognizes edges on the picture (Nobis and Hunziker, 2005). The five rings according to the LAI calculation were used together to calculate the threshold for each picture. By applying this brightness threshold Hemisfer classifies each photograph in either white (sky) or black (vegetation) pixels before estimating the LAI. For hemispherical photographs the proportion of white pixels to the total pixel number corresponds to the gap fraction. The next step was to calculate the average number of times, called the contact number, that a light ray would touch the canopy when travelling a distance equal to the thickness of the canopy

(Hemisfer, 2005). These values are finally integrated over the rings to calculate the LAI, but this step differs among methods (Hemisfer Help). Hemisfer permits the calculation of LAI with five different mathematical methods:

- 1) method by Miller (1967)
- 2) method by Miller (1967) as implemented in the LAI-2000
- 3) method by Lang (1987),
- 4) method by Norman and Campbell (1989)
- 5) weighted ellipsoidal method (developed for Hemisfer).

The ellipsoidal method is similar to Norman & Campbell (1989) but it optimizes the LAI itself rather than the light transmission. LAI was calculated by using all five methods in order to evaluate them. Finally, all LAI-estimates were corrected for clumping based on the method of Chen and Cihlar (1995) that is also implemented into Hemisfer. Only the blue band of the photographs was used in the analysis to minimize the interference of multiple scattering in the canopy (Zhang et al., 2005) and corresponding to the LAI-2000 instrument.

The second instrument used to determine LAI was an LAI-2000 plant canopy analyzer. It measures simultaneously diffuse radiation by means of a fish-eye light sensor in five distinct angular bands, with central zenith angle of 7, 23, 38, 53 and 68°. Only the incoming radiation of less than 490 nm is measured to minimize the radiation scattered by the canopy (LI-COR, 1992). LAI-2000 requires measurements below and above the canopy. The latter samples were measured at the same time in a non-wooded clearing. The ratio of the two values gives the transmittance for each sky sector (Jonckheere et al., 2004). From this ratio the gap fraction can be estimated from which the LAI calculations based on Miller's method (1967) are automatically derived (LI-COR, 1992).

2.3 HyMap Data Acquisition and Preprocessing

Airborne imaging spectrometer data were acquired on July 29, 2004, with HyVista's Hyperspectral Mapping Imaging Spectrometer (HyMap) (Cocks et al., 1998). The HyMap sensor measures radiance from the ground in 126 contiguous wavebands from 450 to 2500 nm with spectral bandwidths of 10–20 nm and a field of view of 61.3°. A total of three 2.5x12 km images were obtained under cloud free conditions at a flight altitude of 3000 m that resulted in a spatial resolution of 5 m (Huber et al., 2007). Two images were orientated North-South and the third was acquired perpendicular to them while the solar azimuth was at ~127.2° and the zenith was at ~38.2°.

The preprocessing of the HyMap data was performed as described by Huber et al. (2007). The geometric correction based on the parametric geocoding procedure PARGE (Schläpfer and Richter, 2002) and radiometric correction was performed with the ATCOR4 software (Richter and Schläpfer, 2002). Additionally, illumination effects were corrected due to the sensors large field of view. As can be seen from Figure 1, a clear trend of decreasing DN values from the left to the right edge of the image was observable before the across-track-illumination correction. The illumination variations were corrected by applying a procedure implemented in the software package ENVI 4.3. The ENVI routine computed along-track mean brightness values for each across-track pixel and displayed these as a series of curves, one for each band of data in the image. Following this, a second-order polynomial function was fitted to each curve, which is used to remove the across-track variation (Taylor, 2001). View angle compensation was conducted by a

multiplicative technique that is also part of the ENVI routine (Research Systems, 2004).

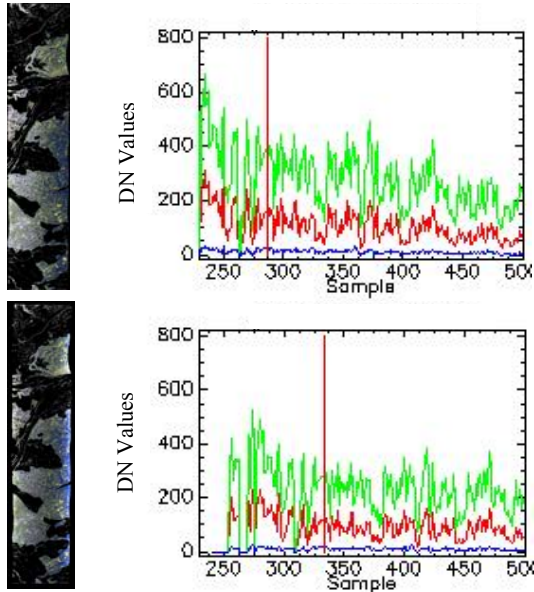


Figure 1. Horizontal reflectance profile before (above) and after (below) the across-track-illumination correction.

2.4 Vegetation indices applied on HyMap Data

Vegetation indices are the main method used to enhance the reflectance signal of vegetation. VI's are originally constructed as functions of red and NIR wavebands. In a recent study, it has been shown that hyperspectral bands in the SWIR region and some in the NIR region have a great potential in forming indices for LAI estimations (Gong et al., 2003; Schlerf et al., 2005). In the SWIR region the liquid water absorption for vegetation is characteristic. Analogously to the study of Hunt (1991), it was hypothesized that the VI's are correlated to the LAI through the summation of the individual leaf equivalent water thicknesses for each leaf layer to obtain a total canopy equivalent water thickness, which can be considered as the depth of water in the foliage (Hunt, 1991).

In this study all three spectral regions (red, NIR, SWIR) were used to calculate VI's. Criteria for selecting the VI's were their performances in forest canopies in previous studies. Table 1 presents the chosen VI's.

Group	Name	Formula	References
Ratio VI	Simple ratio	$SR = \rho_{\lambda 1} / \rho_{\lambda 2}$	(Pearson and Miller, 1972)
Ratio VI	Normalized difference vegetation index	$NDVI = (\rho_{\lambda 1} - \rho_{\lambda 2}) / (\rho_{\lambda 1} + \rho_{\lambda 2})$	(Rouse et al., 1974)
Ratio VI	Non-linear vegetation index	$NLI = (\rho_{\lambda 1}^2 \cdot \rho_{\lambda 2}) / (\rho_{\lambda 1}^2 + \rho_{\lambda 2})$	(Gong et al., 2003)
Orthogonal VI	Perpendicular vegetation index	$PVI = (1/\sqrt{(a^2+1)}) * (\rho_{\lambda 1} - a*\rho_{\lambda 2}-b)$	(Richardson and Wiegand, 1977)

Hybrid VI	Soil adjusted vegetation index	$SAVI = ((\rho_{\lambda 1} - \rho_{\lambda 2})(1+L)) / (\rho_{\lambda 1} + \rho_{\lambda 2} + L)$	(Huete, 1988)
Hybrid VI	Second soil-adjusted vegetation index	$SAVI2 = \rho_{\lambda 1} / (\rho_{\lambda 2} + b/a)$	(Major et al., 1990)

Table 1. Vegetation indices used in this study. ρ stands for reflectance, $\lambda 1$ and $\lambda 2$ are wavelengths and a and b represent the soil line coefficients.

Generally, the VI's can be grouped into: 1) ratio indices, 2) orthogonal indices and 3) hybrid indices. Ratio indices are based on the calculation of quotients of two reflectance values of the spectrum. They are computed independently of soil reflectance properties. Orthogonal indices, in contrast, take soil reflectance properties into account. They assume that the reflectance in the NIR and red varies with increasing vegetation density (such as leaf area index) and that these variations are parallel to the soil baseline. The soil line is representing the relationship between red and NIR soil reflectances and the perpendicular distance from the baseline in a NIR-red plot determines the vegetation density. To define the soil line coefficients of our images a tasselled cap was performed which resulted in a slope of 0.9 and an intercept of 0.1. Hybrid indices can be considered as a mixture between the ratio and the orthogonal indices (Broge and Leblanc, 2000). Hybrid indices were developed to account for changes of the optical properties of the background (Broge and Leblanc, 2000). They include the coefficients of the soil line or a soil-adjustment factor (L) to minimize soil-brightness influences. In this study an adjusted factor of $L = 0.5$ was used which was defined for intermediate vegetation amounts (Huete, 1988).

Before applying equations between field-measured LAI and VI's, we had to extract spectral reflectances from the HyMap data, corresponding to our subplots. To extract the mean spectra of eight subplots from the HyMap images the ENVI Region of Interest Tool was used. Afterwards, HyMap bands were selected from literature to use for the VI's. Only for the Simple Ratio we tried to define our own wavebands. This was done by using all combinations of two wavelengths involving the 126 HyMap bands and correlating them to the LAI obtained from hemispherical photographs acquired with manual exposure. We calculated a correlation matrix for the mean, maximum, minimum and median values of the LAI. In case that measurements of the year 2005 were available these LAI values were used, otherwise we reverted to the LAI values of the year 2006. The results for the mean LAI, which achieved highest R^2 values in this correlation analysis, are presented in Figure 2.

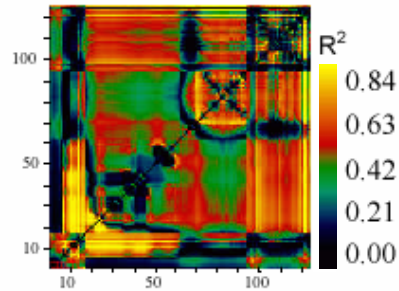


Figure 2. 2D correlation matrix that shows the coefficient of determination (R^2) between LAI obtained from hemispherical photography and narrow band SR.

The hyperspectral bands for the other VI's were chosen based on their performance in previous studies for forest ecosystems. Table 2 presents the wavebands used in our study. Compared to the ones of the publications referenced the wavebands are slightly modified according to the utilized HyMap data.

Index	λ_1 (nm)	λ_2 (nm)	Adjusted R^2	References
SR	1113	1007	0.46	(Gong et al., 2003)
SR	786	635	0.40	Own calculation
NDVI	1038	831	0.67	(Gong et al., 2003)
NLI	1558	844	0.37	(Gong et al., 2003)
PVI	1148	1088	0.78	(Baret and Guyot, 1991; Broge and Leblanc, 2001; Schlerf et al., 2005)
SAVI	1038	831	0.59	(Elvidge and Chen, 1995; Huete, 1988)
SAVI2	725	1953	0.73	(Broge and Leblanc, 2000; Darvishzadeh et al., 2006)

Table 2. The wavelength positions used for calculating VI's. Apart from the second Index Simple Ratio, all positions were taken from the publications referenced.

To find out which Index is most promising for our study area, regression models between LAI, obtained from hemispherical photographs, and the VI's were developed. For comparison of the performance of the regression models, the adjusted R^2 was used. With the best VI's LAI maps for the study area were calculated in order to evaluate illumination effects on LAI when using indices derived from HyMap data.

2.5 Statistical analysis

As a first step, the variance homogeneity of LAI calculation methods was evaluated by applying the F-test ($p < 0.05$) on LAI estimates. This test was computed to determine differences of the variance between the methods. The hypotheses of the F-test are a) there is no difference between the variances and b) the difference between the variances are significantly different. As a next step, the coefficient of variation was calculated. It is a relative measure for comparing the degree of variation from one dataset to another, even if the means are different from each other. The coefficient of variation is defined as the ratio of the standard deviation to the mean multiplied by 100. Statistical evaluations for this study were performed using the R statistical package, a free software environment for statistical computing and graphics (R Development Core Team, 2005) under the GNU public license.

3. RESULTS

In total, 364 hemispherical photographs were processed with Hemisfer, which were taken on five different dates in 2005 and on one date in 2006. Simultaneously, LAI-2000 measurements were collected at one date in both years for direct comparison of the instruments at four subplots. At one subplot LAI-2000 measurements were carried out in both years. Since not all different kinds of measurements were carried out at each subplot and each date, only the according results were used for this analysis.

3.1 LAI calculation methods

Five different mathematical LAI calculation methods were evaluated, which are implemented in the Hemisfer software. The minimum (1.91; manual exposure) and maximum (4.93;

automatic exposure) LAI were found with the method after Norman and Campbell. The F-test revealed that the weighted ellipsoidal method as well as the method according to Norman and Campbell significantly differed to the other three methods (Licor LAI-2000, Lang, Miller). This result was found for both exposure settings. The lowest coefficient of variation was obtained for LAI estimates calculated after Lang (manual: 10.99 %; automatic: 10.67 %) for both exposure settings. The coefficients of variation of the other methods ranged from 11.53 % to 15.43 % for manual exposure and from 10.69 % to 14.26 % for automatic exposure. The boxplots in Figure 3 illustrate these findings. Additionally, it can be seen from Figure 3 that LAI values of 2006 are lower than those in the other years. Considering only the subplots of 2006, the mean LAI estimates were about 10 % lower.

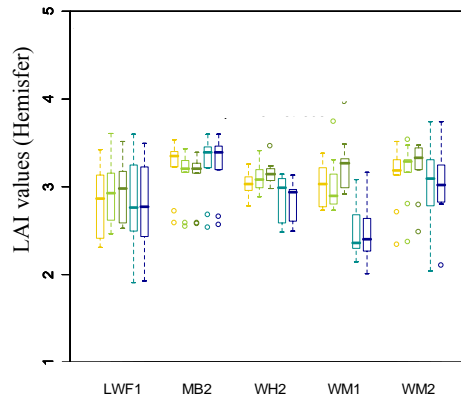


Figure 3. LAI estimates obtained from manually exposed photographs taken at five subplots. LAI were calculated with five different mathematical methods: — LAI-2000 method, — Method Lang, — Method Miller, — Method Norman and Campbell, — weighted ellipsoidal method.

3.2 The influence of camera exposure settings on LAI

In order to investigate the effects of camera light exposure settings on LAI estimates, the hemispherical photographs (only data of 2005 and 2006 and results of the Lang method were taken into account) at each subplot with the two different settings were included in the analysis. A visual comparison of pictures taken with two different settings showed that tree crowns appeared brighter in automatically exposed photographs and with varying green colours than in manually exposed images (Fig. 4).

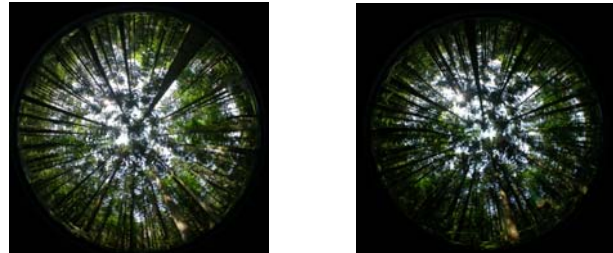


Figure 4. Hemispherical photographs automatically (left) and manually exposed (right).

LAI estimates of photographs obtained with automatic and manual exposure ranged from 2.00 to 4.93 and from 1.91 to 4.49, respectively. The mean LAI of all methods were compared to determine the influence of exposure on LAI estimates. These results illustrate that hemispherical photographs acquired with automatic exposure underestimate the LAI by 10 %.

LAI estimates obtained from manually exposed pictures exhibited a larger variability than those obtained from automatically exposed photographs for all calculation methods (Fig. 4).

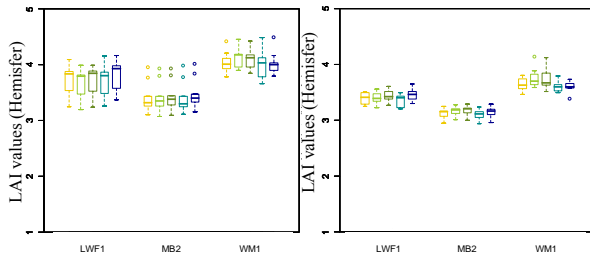


Figure 5. LAI based on photographs of July 15, 2005 for manual exposure (left) and automatic exposure setting (right) for three subplots (— Li-Cor LAI-2000 method, — Method according to Lang, — Method according to Miller, — Method according to Norman and Campbell, — weighted ellipsoidal method).

Further analysis included to test which exposure setting is the most favourable for LAI estimation. LAI derived from hemispherical photographs of the years 2005 and 2006 (only results according to Licor LAI-2000 method) were compared to LAI-2000 measurements taken at the same subplots. The LAI-2000 measurements ranged from 2.93 to 4.19. LAI estimates obtained from hemispherical photographs with automatic exposure correlated not as good with LAI-2000 measurements ($R^2 = 0.85$, $RMSE = 0.16$) as LAI estimates based on manual exposure ($R^2 = 0.97$, $RMSE = 0.10$).

3.3 Evaluation of illumination effects on LAI estimates

The evaluation of illumination effects on LAI estimates derived with VI from HyMap data were based on the analysis of continuous LAI estimates. To assess spatial LAI estimates, linear regression models between ground-based LAI and each VI were evaluated. LAI calculated after Lang from manually exposed hemispherical photographs for calibration were used. The formulas in Table 1 were used to compute the VI values. For the SR, the correlation matrix shows mainly high R^2 values for two bands in the Red and NIR region (for example band 14 (635 nm) and 24 (786 nm)), but also in the SWIR region good correlations were found (for example band 104 (2119 nm) and 121 (2404 nm)).

The best linear relationship was achieved for PVI ($R^2 = 0.78$, $RMSE = 0.16$). Thus, we applied the equation based on PVI on all HyMap images to obtain spatial LAI maps. On the HyMap image that was West-East oriented, the mean LAI of the upper and lower edge were compared to determine the illumination effects on LAI estimates. LAI values of the upper

edge of the image showed 8 % higher values than those of the lower edge. Further comparisons indicated that LAI obtained of the West-East image agreed better with the LAI obtained with hemispherical photography than those obtained with the North-South oriented image.

4. DISCUSSION AND CONCLUSIONS

This project was undertaken 1) to evaluate five different LAI calculation methods, 2) to investigate the influence of camera exposure settings on LAI estimates and 3) to examine illumination effects on LAI when using VI's applied on HyMap data.

The comparison of five different LAI calculation methods exposed differences among the methods on a subplot level. However, if mean values of several subplots were compared, these differences were reduced. The observed decrease for the year 2006 compared to the other years could be attributed to different weather conditions and therefore also to diverse illumination conditions. This decrease was found for all subplots. Previous studies have mentioned the importance of illumination condition at acquisition time and recommended diffuse conditions as the most advantageous. However, field campaigns cannot always be conducted under ideal conditions. Because the conditions were not identical at the different sampling dates, results have to be interpreted with care. On the question of the most robust LAI calculation method, the findings of this study indicated that the method by Lang is the most robust method what is consistent with Schleppe et al. (2007).

The second objective was the investigation of exposure influencing LAI estimates. Increased exposure, as used with automatic light exposure, resulted in decreasing shutter speeds and increasing image brightness (Zhang et al., 2005). Canopy gaps in photographs acquired with automatic light exposure are visually larger than those in the counterpart, thus resulting in an overestimation of gap fraction and an underestimation of LAI estimations (Zhang et al., 2005). Comparison of the LAI-2000 values and the LAI estimates obtained from manually exposed photographs correlated better than automatically exposed photographs. Hence, it seems that the manual exposure is the better choice for retrieving LAI with hemispherical photography. However, these data must be interpreted with caution because of the small sample size. The relevance of accurate exposure is clearly supported by our findings and they are in agreement with the study of Zhang et al. (2005) who determined the optimum exposure.

Finally, we examined the influence of illumination effects in HyMap data on LAI when using VI's. Although an illumination correction was performed before applying VI's, a visible examination of the images showed strong effects at the edges of all three images. In the HyMap scene flown from West to East, higher LAI values at the upper edge of the image were obtained. A possible explanation for this might be that the whiskbroom sensor with a large field of view (61.3°) resulted in higher reflectances due to strong backward scattering of the vegetation.

References

- Baret, F. and Guyot, G., 1991. Potentials and Limits of Vegetation Indexes for LAI and ARA Assessment. *Remote Sensing of Environment*, 35(2-3), pp. 161-173.
- Baret, F. et al., 2006. VALERI: A network of sites and a methodology for the validation of medium spatial

- resolution satellite products. *Remote Sensing of Environment*, Submitted for publication, pp.
- Broge, N.H. and Leblanc, E., 2000. Comparing prediction power and stability of broadband and hyperspectral vegetation indices for estimation of green leaf area index and canopy chlorophyll density. *Remote Sensing of Environment*, 76(2), pp. 156-172.
- Broge, N.H. and Leblanc, E., 2001. Comparing prediction power and stability of broadband and hyperspectral vegetation indices for estimation of green leaf area index and canopy chlorophyll density. *Remote Sensing of Environment*, 76(2), pp. 156-172.
- Chen, J.M. and Black, T.A., 1992. Defining Leaf-Area Index for Non-Flat Leaves. *Plant Cell and Environment*, 15(4), pp. 421-429.
- Chen, J.M. and Cihlar, J., 1995. Quantifying the Effect of Canopy Architecture on Optical Measurements of Leaf-Area Index Using 2 Gap Size Analysis-Methods. *Ieee Transactions on Geoscience and Remote Sensing*, 33(3), pp. 777-787.
- Cocks, T. et al., 1998. The HyMap™ airborne hyperspectral sensor: the system, calibration and performance. In: *1st EARSeL Workshop on Imaging Spectroscopy*. EARSeL, Zurich.
- Darvishzadeh, R. et al., 2006. Hyperspectral vegetation indices for estimation of leaf area index. In: *ISPRS Commission VII Mid-term Symposium 8-11 May 2006*, Enschede, the Netherlands.
- Elvidge, C.D. and Chen, Z.K., 1995. Comparison of Broad-Band and Narrow-Band Red and near-Infrared Vegetation Indexes. *Remote Sensing of Environment*, 54(1), pp. 38-48.
- Gong, P. et al., 2003. Estimation of forest leaf area index using vegetation indices derived from Hyperion hyperspectral data. *Ieee Transactions on Geoscience and Remote Sensing*, 41(6), pp. 1355-1362.
- Hemisfer, 2005. Hemisfer 1.3 Online Help.
- Huber, S. et al., 2007. Estimating Biochemistry in Mixed Forests from HyMap Data using Band-Depth Analyses and Subset Regression Algorithms. In Preparation, pp.
- Huete, a.R., 1988. A Soil-Adjusted Vegetation Index (Savi). *Remote Sensing of Environment*, 25(3), pp. 295-309.
- Hunt, E.R., 1991. Airborne Remote-Sensing of Canopy Water Thickness Scaled from Leaf Spectrometer Data. *International Journal of Remote Sensing*, 12(3), pp. 643-649.
- Jonckheere, I. et al., 2004. Review of methods for in situ leaf area index determination - Part I. Theories, sensors and hemispherical photography. *Agricultural and Forest Meteorology*, 121(1-2), pp. 19-35.
- Leblanc, S.G. et al., 2005. Methodology comparison for canopy structure parameters extraction from digital hemispherical photography in boreal forests. *Agricultural and Forest Meteorology*, 129(3-4), pp. 187-207.
- LI-COR, 1992. LAI-2000 Plant Canopy Analyser. Instruction manual. LICOR, Lincoln, NE, USA.
- Major, D.J. et al., 1990. A Ratio Vegetation Index Adjusted for Soil Brightness. *International Journal of Remote Sensing*, 11(5), pp. 727-740.
- Miller, J.B., 1967. A Formula for Average Foliage Density. *Australian Journal of Botany*, 15(1), pp. 141-&.
- Nikon Inc., 2002. CoolPix 4500. <http://www.nikonusa.com/template.php?cat=1&grp=2&productNr=25503> (assessed 15 March 2007).
- Nobis, M. and Hunziker, U., 2005. Automatic thresholding for hemispherical canopy-photographs based on edge detection. *Agricultural and Forest Meteorology*, 128(3-4), pp. 243-250.
- Pearson, R.L. and Miller, L.D., 1972. Remote Mapping of standing crop biomass for estimation of the productivity of the short-grass prairie, Pawnee National Grasslands, Colorado. In: *8th International Symposium on Remote Sensing of Environment*. ERIM International, Ann Arbor, Mich.
- R Development Core Team, 2005. R: A language and environment for statistical computing. R Foundation for Statistical Computing., Vienna, Austria.
- Research Systems, 2004. ENVI User's Guide. Research Systems Inc.
- Rich, P.M., 1990. Characterizing Plant Canopies with Hemispherical Photographs. *Remote Sensing Reviews*, 5(1), pp. 13-29.
- Richardson, a.J. and Wiegand, C.L., 1977. Distinguishing Vegetation from Soil Background Information. *Photogrammetric Engineering and Remote Sensing*, 43(12), pp. 1541-1552.
- Richter, R. and Schlaepfer, D., 2002. Geo-atmospheric processing of airborne imaging spectrometry data. Part 2: atmospheric/topographic correction. *International Journal of Remote Sensing*, 23(13), pp. 2631-2649.
- Rouse, J.W. et al., 1974. Monitoring the vernal advancement of retrogradation of natural vegetation. In: *NASA/GSFC, type III, final report (pp. 1-371)*, Greenbelt, MD, USA.
- Schleppi, P. et al., 2006. Correcting non-linearity and slope effects in the estimation of the leaf area index of forests from hemispherical photographs. *Agricultural and Forest Meteorology*, Submitted, pp.
- Schlerf, M. et al., 2005. Remote sensing of forest biophysical variables using HyMap imaging spectrometer data. *Remote Sensing of Environment*, In Press, Corrected Proof, pp.
- Schläpfer, D. and Richter, R., 2002. Geo-atmospheric processing of airborne imaging spectrometry data. Part 1: parametric orthorectification. *International Journal of Remote Sensing*, 23(13), pp. 2609-2630.
- Taylor, G., 2001. Strategies for Overcoming Problems when Mosaicking Airborne Scanner Images. *Earth Observation Magazine*, 10(8), pp.
- van Gardingen, P.R. et al., 1999. Leaf area index estimates obtained for clumped canopies using hemispherical photography. *Agricultural and Forest Meteorology*, 94(3-4), pp. 243.
- Zhang, Y. et al., 2005. Determining digital hemispherical photograph exposure for leaf area index estimation. *Agricultural and Forest Meteorology*, 133(1-4), pp. 166.